

Trifluoromethylation of Anthraquinones for n-Type Organic Semiconductors in Field Effect Transistors

Mengna Zhao, Xinkan Yang, Gavin Chit Tsui, and Qian Miao

J. Org. Chem., **Just Accepted Manuscript** • DOI: 10.1021/acs.joc.9b01263 • Publication Date (Web): 16 Jul 2019

Downloaded from pubs.acs.org on July 17, 2019

Just Accepted

“Just Accepted” manuscripts have been peer-reviewed and accepted for publication. They are posted online prior to technical editing, formatting for publication and author proofing. The American Chemical Society provides “Just Accepted” as a service to the research community to expedite the dissemination of scientific material as soon as possible after acceptance. “Just Accepted” manuscripts appear in full in PDF format accompanied by an HTML abstract. “Just Accepted” manuscripts have been fully peer reviewed, but should not be considered the official version of record. They are citable by the Digital Object Identifier (DOI®). “Just Accepted” is an optional service offered to authors. Therefore, the “Just Accepted” Web site may not include all articles that will be published in the journal. After a manuscript is technically edited and formatted, it will be removed from the “Just Accepted” Web site and published as an ASAP article. Note that technical editing may introduce minor changes to the manuscript text and/or graphics which could affect content, and all legal disclaimers and ethical guidelines that apply to the journal pertain. ACS cannot be held responsible for errors or consequences arising from the use of information contained in these “Just Accepted” manuscripts.

Trifluoromethylation of Anthraquinones for n-Type Organic Semiconductors in Field Effect Transistors

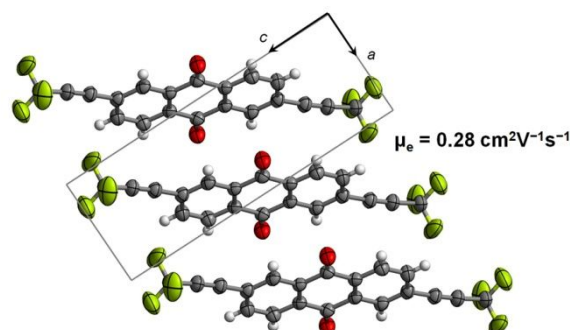
Mengna Zhao, Xinkan Yang, Gavin Chit Tsui*, Qian Miao*

Department of Chemistry, The Chinese University of Hong Kong, Shatin, New Territories,
Hong Kong, China

* gctsui@cuhk.edu.hk, miaoqian@cuhk.edu.hk

Abstract

This study puts forth a new design of n-type organic semiconductors, which has trifluoromethylethynyl groups attached to 9,10-anthraquinone at different positions. These electron-deficient anthraquinones are synthesized by trifluoromethylation of the corresponding trimethylsilyl-protected alkynes with fluoroform-derived CuCF_3 , and their π - π stacking in the crystals is tunable by varying the positions of trifluoromethylethynyl groups. It is found that most of these trifluoromethylated anthraquinones function as n-type semiconductors in solution-processed field effect transistors with electron mobility of up to $0.28 \text{ cm}^2 \text{ V}^{-1} \text{ s}^{-1}$.



Introduction

Herein we demonstrate that trifluoromethylation of anthraquinone derivatives results in novel n-type organic semiconductors, which exhibit field effect mobility of up to 0.28 cm²/Vs in solution-processed organic field effect transistors (OFETs). OFETs are one of the most important elemental devices of organic semiconductors for a variety of applications in light-weight, low-cost, flexible and wearable electronics.¹ Low-power complementary circuits require both p- and n-channel OFETs as elemental units, which are based on p- and n-type organic semiconductors, respectively. Despite recent significant progress in n-channel OFETs² with field effect mobility exceeding 10 cm²/Vs,^{3, 4, 5} n-type organic semiconductors are still underdeveloped in comparison to their p-type counterparts,⁶ partially due to the inherent instability of organic anions, particularly, in the presence of air and water. When developing new n-type organic semiconductors that combine high field effect mobility, robust environmental stability and easy processability, one challenge is that only a handful of electron-deficient π -building blocks are available for molecular design and even fewer have been demonstrated to lead to high-mobility n-channel OFETs.⁷ To meet this challenge, we explored a new design for n-type semiconductors in this study by attaching trifluoromethyl groups to 9,10-anthraquinone through an ethynyl linker. Quinones are well known electron acceptors in organic synthesis and biological systems, but have been rarely explored for development of n-type organic semiconductors.^{8, 9, 10} Trifluoromethyl was used as an electron-withdrawing substituent for developing n-type organic semiconductors, where 4-trifluoromethylphenyl groups were attached to π -backbones.^{9, 10, 11} The lowest unoccupied molecular orbital (LUMO) energy level of 9,10-anthraquinone is calculated as -3.22 eV. As found from this study, attachment of two trifluoromethylethynyl groups to 9,10-anthraquinone at different positions can not only lower the calculated LUMO energy level significantly to -3.82 ~ -3.96 eV but also tune molecular packing in the solid state,

which is of key importance to charge transport in organic semiconductors. Detailed below are the synthesis, molecular packing and solution-processed OFETs of trifluoromethylethynylated anthraquinones **1a–d** (Figure 1).

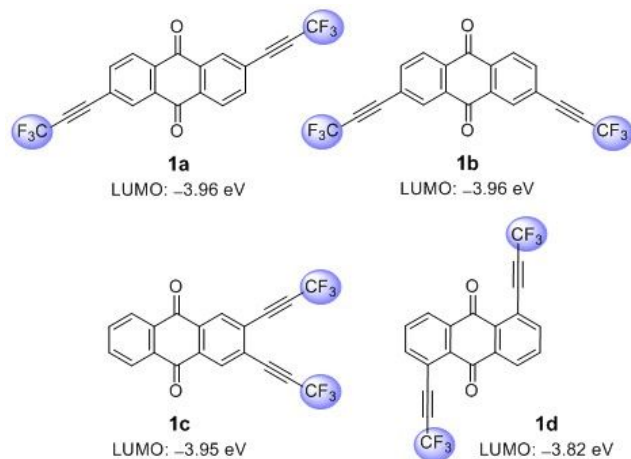


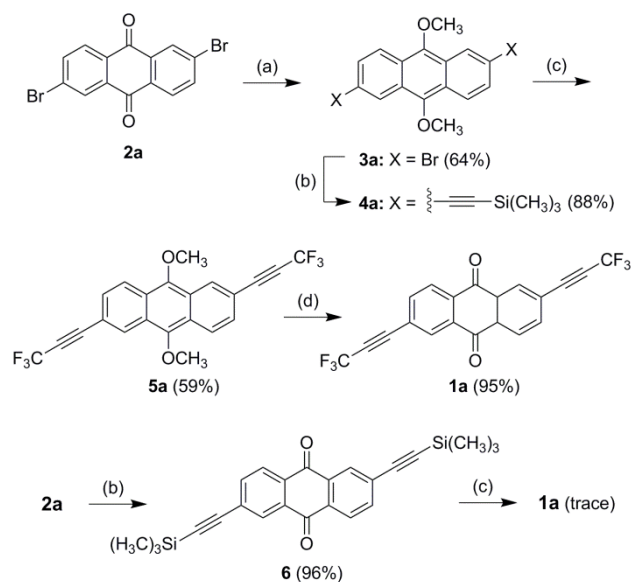
Figure 1 Bis(trifluoromethylethynyl)-9,10-anthraquinones (**1a–d**) with the LUMO energy levels, which are calculated at the B3LYP level of density functional theory (DFT) with the 6-311++G(d,p) basis set.

Results and Discussion

Scheme 1 shows the synthesis of **1a** from 2,5-dibromo-9,10-anthraquinone (**2a**)¹² in four steps. Reduction of **2a** with sodium dithionite followed by methylation¹³ gave 2,5-dibromo-9,10-dimethoxyanthracene (**3a**), and the Sonogashira coupling of **3a** with trimethylsilylacetylene gave diethynylated anthracene **4a** in a yield of 88%. Subsequent reaction of **4a** with fluoroform-derived CuCF_3 ¹⁴ using the reported method¹⁵ enabled trifluoromethylation of the trimethylsilyl-protected alkynes to afford **5a** in a yield of 59%. Final oxidation of **5a** by NBS¹⁶ resulted in trifluoromethylated anthraquinone **1a** in a yield of 95%. In contrast, our attempts to trifluoromethylate anthraquinone **6** with fluoroform-derived CuCF_3 using the same procedure only gave a trace amount of **1a**, which was identified with ^1H and ^{19}F NMR. This failure is presumably related to the electron-deficient nature of **6**. In a

similar way, other trifluoromethylated anthraquinones (**1b–d**) were synthesized in four steps from the corresponding dihalo-9,10-anthraquinones as shown in Scheme S1–3 in the Supporting Information.

Scheme 1 Synthesis of **1a**



Reagents and conditions: (a) Na₂S₂O₄, NaOH, tetrabutylammonium bromide, CH₃I, CH₂Cl₂, H₂O; (b) trimethylsilylacetylene, Pd(PPh₃)₄, CuI, diisopropylamine, THF, reflux; (c) [CuCF₃], TMEDA, DMF; (d) NBS, THF, H₂O.

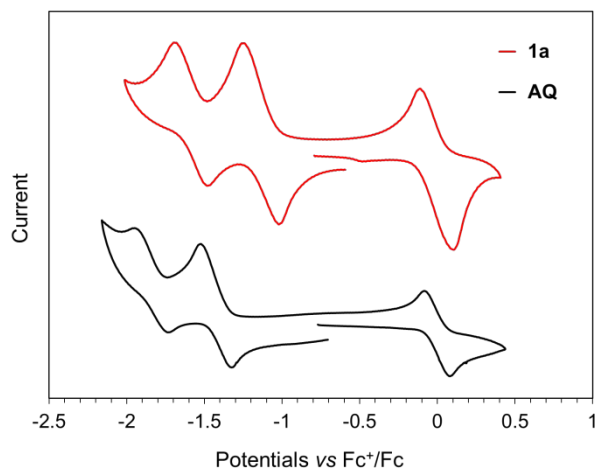
The electrochemical and optical properties of **1a–d**, in comparison with those of 9,10-anthraquinone (AQ), were studied with cyclic voltammetry (CV) and UV-vis absorption spectroscopy, respectively. In the test window of CV, **1a–d** all exhibited two quasi-reversible reduction waves but did not exhibit any oxidation waves. Figure 2 compares the cyclic voltammograms of **1a** and AQ, and Figure S1 in the Supporting Information shows the cyclic voltammograms of **1b–d**. As shown in Table 1, the first reduction waves of **1a–d** have half-wave potentials in the range of -1.20 V to -1.11 V *versus* ferrocenium/ferrocene (Fc⁺/Fc), which are more positive than that of AQ by 0.23 V to 0.32 V. In comparison to **1a**,

1
2
3 2,6-bis(4-(trifluoromethyl)phenyl)-9,10-anthraquinone was reported to have a half-wave
4 reduction potential of -0.88 V versus SCE,⁹ which is equivalent to -1.28 V versus Fc⁺/Fc.
5
6 This indicates that trifluoromethylethynyl is more effective than 4-(trifluoromethyl)phenyl in
7 lowering LUMO energy level of anthraquinone presumably due to the extra
8 electron-withdrawing ability of *sp* carbons in the ethynyl group. On the basis of the first
9 reduction potentials, the LUMO energy levels of **1a–d** are estimated as -3.90 eV to -3.99
10 eV ,¹⁷ in good agreement with the DFT calculated values. Quinones **1a–d** are all pale-yellow
11 solids, which form essentially colorless solutions in CH₂Cl₂. The solutions of **1a–c** in CH₂Cl₂
12 exhibit very similar absorption spectra with three sets of absorption band in the UV region,
13 while the absorption band of **1d** is broader and less structured with a slightly red-shifted
14 absorption edge as shown in Figure S2 in the Supporting Information. On the basis of the
15 absorption edge, the optical gaps of **1a–d** are estimated as wide as 3.28 to 3.43 eV. The fact
16 that **1a–c** have essentially the same LUMO energy levels and **1d** has a slightly higher LUMO
17 energy level indicates that the substitution position of trifluoromethylethynyl groups plays a
18 very minor role in withdrawing electrons from the anthraquinone backbone.
19
20
21
22
23
24
25
26
27
28
29
30
31
32
33
34
35
36
37
38
39
40
41
42
43
44
45
46
47
48
49
50
51
52
53
54
55
56
57
58
59
60

Table 1 The electrochemical and optical properties of anthraquinones.

	Experimental				Calculated	
	E_{red}^1	E_{red}^2	LUMO	λ_{edge}	LUMO	HOMO
	(V) ^a	(V) ^a	(eV) ^b	(nm) ^c	(eV) ^d	(eV) ^d
1a	-1.12	-1.58	-3.98	361	-3.96	-7.82
1b	-1.11	-1.57	-3.99	369	-3.96	-7.83
1c	-1.12	-1.67	-3.98	367	-3.95	-7.83
1d	-1.20	-1.72	-3.90	378	-3.82	-7.67
AQ	-1.43	-1.84	-3.67	355	-3.22	-7.41

a. Half-wave potential versus Fc^+/Fc . b. Estimated from $\text{LUMO} = -5.10 - E_{\text{red}}^1$ (eV). c. absorption edge from a 1×10^{-5} M solution in CH_2Cl_2 . d. Calculated at the B3LYP level of DFT with 6-311++G(d, p) basis set.

**Figure 2** Cyclic voltammograms of **1a** and 9,10-anthraquinone (AQ) recorded in CH_2Cl_2 with Fc^+/Fc as the internal standard.

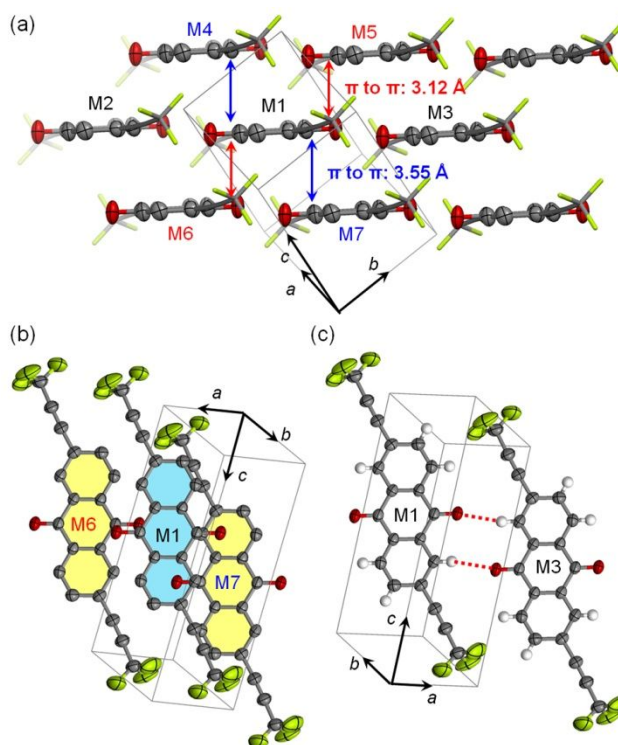


Figure 3 Crystal structure of **1a**: (a) brickwork arrangement; (b) π -overlap (the top molecule is shown in light blue and the bottom molecules are shown in light yellow); (c) weak hydrogen bonds. (C and O atoms are shown as ellipsoids at the 50% probability level; the trifluoromethylethynyl substituents in (a) are shown as sticks; and hydrogen atoms in (a) and (b) are removed for clarity.)

Single crystals of **1a**, **1c** and **1d** qualified for X-ray crystallography were obtained by slow diffusion of ethyl acetate vapor into the solution in chloroform, while the crystals of **1b** obtained with the same method had low quality. Figure 3a shows the crystal structure of **1a**, where molecules of **1a** are packed in a brickwork arrangement as viewed along the long axis of anthraquinone. Each molecule is stacked with four adjacent molecules with two different π - π distances, 3.12 and 3.55 Å. As shown in Figure 3b, the π -overlap between molecules M1 and M6, which have a smaller π - π distance, occurs mainly between the carbonyl groups and results in three intermolecular C-C contacts as short as 3.46 to 3.50 Å between the edges of

1
2
3 anthraquinone. The π -overlap between molecules M1 and M7 occurs between the edges of
4 anthraquinone as well as ethynyl groups, resulting in four intermolecular C-C contacts of
5 3.54 to 3.67 Å. As shown in Figure 3c, neighboring π -stacks of **1a** are separated by short
6 H \cdots O contacts (2.40 Å), which are shorter than the sum of the van der Waals radii of H and
7 O atoms (2.72 Å). This intermolecular H \cdots O contact can be considered as a weak H-bond
8 since its C-H \cdots O angle (166.0°) is close to 180°.
9

10
11
12 Similarly, **1c** in crystals also exhibits a brickwork arrangement as viewed along the
13 long axis of anthraquinone as shown in Figure 4a. However, unlike **1a**, the adjacent π -planes
14 of **1c** are not parallel to each other but form a dihedral angle of 13.06°. Each molecule (e.g.
15 M1) is stacked with four adjacent molecules (e.g. M4, M5, M6 and M7), resulting two
16 patterns of π -overlap as shown in Figure 4b. The π -overlap between molecules M1 and M6
17 occurs between the edges of anthraquinone as well as ethynyl groups, resulting in
18 intermolecular C-C contacts of 3.55 to 3.64 Å. The π -overlap between molecules M1 and M7
19 occurs mainly between the carbonyl groups and results in three intermolecular C-C contacts
20 as short as 3.50 to 3.52 Å between the edges of anthraquinone. Similar to **1a**, **1c** also exhibits
21 weak H-bonds as shown with dashed red lines in Figure 4c, where the H-to-O distance is 2.46
22 to 2.48 Å and the C-H \cdots O angle 149.5 to 151.9°.
23
24
25
26
27
28
29
30
31
32
33
34
35
36
37
38
39
40
41
42
43
44
45
46
47
48
49
50
51
52
53
54
55
56
57
58
59
60

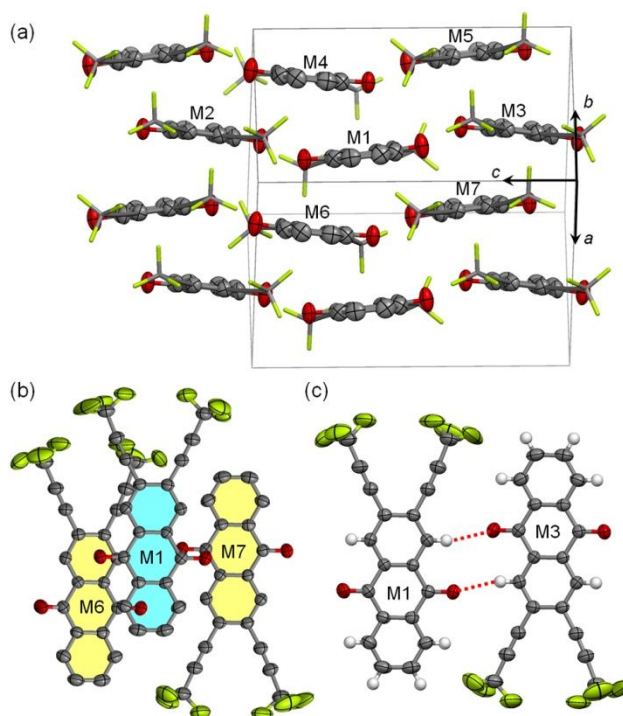


Figure 4 Crystal structure of **1c**: (a) brickwork arrangement; (b) π -overlap (the top molecule is shown in light blue and the bottom molecules are shown in light yellow); (c) weak hydrogen bonds. (C and O atoms are shown as ellipsoids at the 50% probability level; the trifluoromethylethynyl substituents in (a) are shown as sticks; and hydrogen atoms in (a) and (b) are removed for clarity.)

Unlike **1a** and **1c**, **1d** exhibits one-dimensional π - π stacking with two slightly different π - π distances, 3.46 and 3.52 Å, as shown in Figure 5a. The two molecules of **1d** separated by 3.52 Å (e.g. M4 and M5) exhibit larger overlap than those separated by 3.46 Å (e.g. M1 and M2) as shown in Figure 5b. Weak H-bonds similar to those of **1a** and **1c** are not found in the crystal structure of **1d**. The crystal structures of **1a**, **1c** and **1d** indicate that varying the positions of two trifluoromethylethynyl groups that attached to 9,10-anthraquinone enables fine tuning of the π -stacking motifs, in particular, the degree of π -overlap, in the crystals.

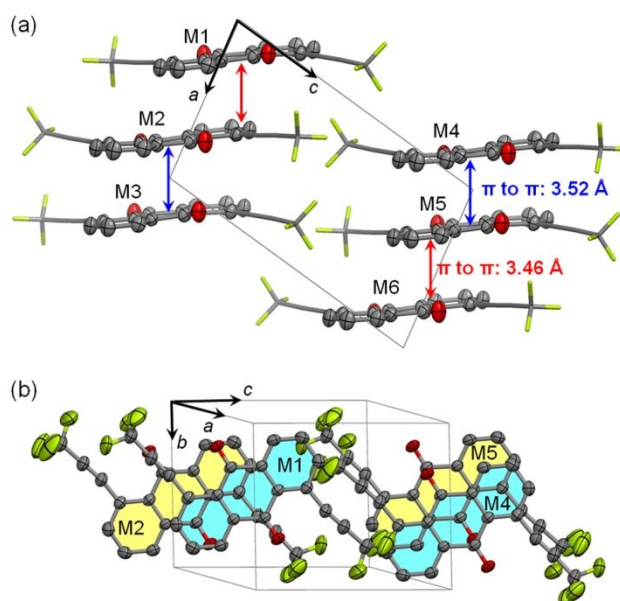


Figure 5 Crystal structure of **1d**: (a) 1D π -stacking as viewed along the b axis; (b) π -overlap (the top molecule is shown in light blue and the bottom molecules are shown in light yellow). (C and O atoms are shown as ellipsoids at the 50% probability level; the trifluoromethylethynyl substituents in (a) are shown as sticks; and hydrogen atoms are removed for clarity).

The low-lying LUMO energy levels and π - π interactions found in the single crystals suggest that **1a–d** can function as n-type organic semiconductors in the solid state. To test their potential semiconductor properties in OFETs, thin films of **1a–d** were deposited by two solution-based methods, namely, drop-casting and dip-coating, onto a silicon substrate, which had successive layers of thermally grown silica, alumina, and 12-cyclohexyldodecylphosphonic acid (CDPA) as a composite dielectric material.⁴ Here, CDPA formed a self-assembled monolayer (SAM) on alumina to passivate surface hydroxyl groups and to provide an ordered dielectric surface wettable by common organic solvents¹⁸ and the resulting CDPA- $\text{AlO}_x/\text{SiO}_2$ had a capacitance per unit area (C_i) of 26 ± 1 nF/cm². It was found that dip-coating resulted in better films of **1a** and **1b**, while drop-casting resulted

1
2
3 in better films of **1c** and **1d**. As observed from polarized-light micrographs and atomic force
4 micrographs shown in Figure S7 and S8 (Supporting Information), **1a** formed isolated
5 crystals larger than 0.2 mm×0.1 mm, while **1b–d** formed continuous films consisting of
6 crystalline fibers or ribbons that are about 1 to 10 μm wide. The crystals of **1a** are in fact
7 single crystals as indicated by the fact that rotating the crystal by 45° under cross-polarized
8 light led to extinction. X-ray diffraction from the film of **1a** exhibited a strong peak at $2\theta =$
9 12.39° (d spacing of 7.15 Å), in accordance with the (002) diffraction as derived from the
10 single crystal structure as shown in Figure S9 in the Supporting Information. Similarly, the
11 film of **1c** exhibited two diffraction peaks corresponding to the (100) and (200)
12 crystallographic planes of the single crystal; and the film of **1d** exhibited three diffraction
13 peaks corresponding to the (001), (002) and (003) crystallographic planes of the single crystal.
14 These diffractions indicate lamellar structures in the films with the corresponding
15 crystallographic planes parallel to the substrate surface. Therefore, it can be concluded that
16 **1a**, **1c** and **1d** all favor an edge-on orientation on the surface as shown in Figure S10 in the
17 Supporting Information. X-ray diffraction from the film of **1b** also exhibited two strong at 2θ
18 $= 9.78^\circ$ and 24.57° , which indicate an ordered arrangement of molecules in the film but
19 cannot provide information about molecular orientation due to lack of single crystal
20 structures.
21
22
23
24
25
26
27
28
29
30
31
32
33
34
35
36
37
38
39
40
41
42
43
44

45 The fabrication of OFETs was completed by depositing a layer of gold on the organic
46 films through a shadow mask to form top-contact source and drain electrodes. In particular, a
47 needle-shaped organic crystal¹⁹ was used as the shadow mask for fabricating single-crystal
48 transistors of **1a**. When measured under vacuum, the crystals of **1a** and the films of **1b** and **1d**
49 all functioned as n-type semiconductors, while the films of **1c** were essentially insulating
50 without field effect. Table 2 summarizes the device performance of **1a–d**, and Figure 6 shows
51 the transfer curve of the best performing device of **1a**, from which a field effect mobility of
52
53
54
55
56
57
58
59
60

0.28 cm²/Vs for electron is extracted. The fact that **1b** and **1d** have a lower electron mobility than **1a** can be attributed to the polycrystalline films of **1b** and **1d**, where charge transport is limited by grain boundaries. The relatively high mobility of **1a** also benefits from a favorable alignment of molecules on the surface (Figure S10a in the Supporting Information), which allows the direction of π - π stacking parallel to the surface, although the degree of π -overlap in the crystals is small. On the other hand, why the films of **1c** did not exhibit field effect remains an unanswered question.

Table 2 Electron mobility (μ_e), on/off ratio (I_{on}/I_{off}) and threshold voltage (V_{th}) of OFETs of **1a–d**.^a

	μ_e (cm ² /Vs)	I_{on}/I_{off}	V_{th} (V)
1a	0.087 ± 0.072	10 ⁴ – 10 ⁵	24–30
	highest: 0.28		
1b	0.029±0.010	10 ³ –10 ⁴	22–26
	highest: 0.042		
1c	No field effect	–	–
1d	4.5±2.0×10 ⁻⁴	10 ² – 10 ³	24–28
	highest: 2.1×10 ⁻³		

^a Electrical measurements were conducted under vacuum and data collected from more than 30 channels on more than 6 substrates for each compound.

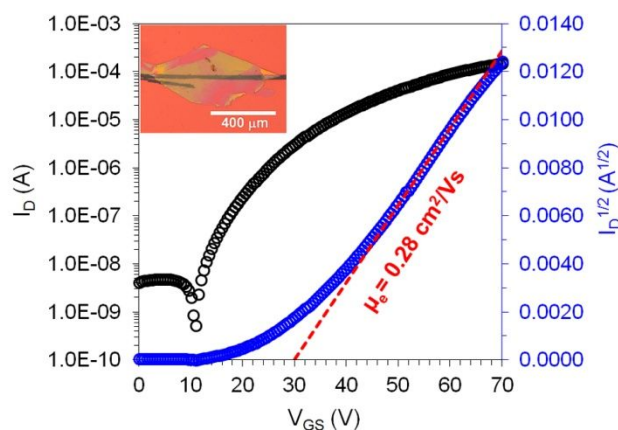


Figure 6 Transfer curve for the best-performing OFET of **1a** on CDPA-modified substrates measured under vacuum with a photograph for the device (channel width: 670 μm , channel length: 24 μm).

Conclusion

In summary, four trifluoromethylethynylated anthraquinones (**1a–d**) were designed as new n-type organic semiconductors and synthesized by trifluoromethylation of the corresponding trimethylsilyl-protected alkynes with fluoroform-derived CuCF_3 . It is found that their π - π stacking in the crystals is tunable by varying the positions of trifluoromethylethynyl groups. These trifluoromethylated anthraquinones except **1c** all behaved as n-type semiconductors in solution-processed field effect transistors, and **1a** exhibited electron mobility of up to $0.28 \text{ cm}^2 \text{ V}^{-1} \text{ s}^{-1}$. This study suggests that late-stage trifluoromethylation is a promising way to develop novel n-type semiconductors.

Experimental Section

Synthesis

General: The reagents and starting materials employed were commercially available and used without any further purification if not specified elsewhere. Anhydrous and O_2 -free THF and CH_2Cl_2 were purified by an Advanced Technology Pure-Solv PS-MD-4 system. For reactions that required heating, the heat source was oil bath. $^1\text{H-NMR}$ (400 MHz), $^{13}\text{C}\{^1\text{H}\}$ -NMR (100 MHz) or $^{19}\text{F-NMR}$ (376 MHz) spectra were recorded on a Bruker

1
2
3 AVANCE III spectrometer. Chemical shift values (δ) are expressed in parts per million using
4 residual solvent peaks ($^1\text{H-NMR}$, $\delta_{\text{H}} = 7.26$ for CDCl_3 ; $^{13}\text{C}\{^1\text{H}\}$ -NMR, $\delta_{\text{C}} = 77.16$ for CDCl_3)
5
6 as internal reference. Chemical shifts of $^{19}\text{F-NMR}$ are reported using benzotrifluoride (-63.72
7
8 ppm) as internal standard. Mass spectra were recorded on a Thermo Finnigan MAT 95 XL
9
10 spectrometer, Bruker 9.4T FTICR MS (solarix) spectrometer, or Bruker Autoflex speed
11
12 MALDI-TOF MS spectrometer. Melting points were measured using a Nikon Polarizing
13
14 Microscope ECLIPSE 50i POL equipped with an INTEC HCS302 heating stage without
15
16 calibration.
17
18
19
20
21

22 **2,6-Dibromo-9,10-dimethoxyanthracene (3a)** ¹³

23
24
25 2,6-Dibromo-9,10-anthraquinone (**2a**) ¹² (400 mg, 1.1 mmol, 1 eq) and
26
27 tetrabutylammonium bromide (354 mg, 1.1 mmol, 1 eq) were dissolved in 15 mL of CH_2Cl_2 .
28
29 To this solution was added a solution of $\text{Na}_2\text{S}_2\text{O}_4$ (432 mg, 2.48 mmol, 2.25 eq) and 1.5 g of
30
31 NaOH in 7.5 mL of water under an atmosphere of N_2 , and the resulting mixture was stirred
32
33 for 2 h at room temperature. After slow addition of methyl iodide (0.7 mL, 11 mmol, 10 eq)
34
35 via a syringe, the mixture was stirred at room temperature under an atmosphere of N_2 for
36
37 another 8 h and then extracted with CH_2Cl_2 . The combined organic layers were washed with
38
39 water and brine, dried over anhydrous Na_2SO_4 , and concentrated under reduced pressure. The
40
41 product was purified by column chromatography using hexane/ CH_2Cl_2 (4/1, v/v) as the eluent,
42
43 yielding 275 mg (0.70 mmol, 64%) of **3a** as a yellow solid. $^1\text{H-NMR}$ (400 MHz, CDCl_3): $\delta =$
44
45 8.43 (d, $^4J(\text{H}, \text{H}) = 1.6$ Hz, 2H), 8.16 (d, $^3J(\text{H}, \text{H}) = 9.2$ Hz, 2H), 7.57 (dd, $^3J(\text{H}, \text{H}) = 9.2$ Hz,
46
47 $^4J(\text{H}, \text{H}) = 2$ Hz, 2H), 4.09 (s, 6H) ppm. The $^1\text{H-NMR}$ data are consistent with the reported. ¹³
48
49
50
51
52
53
54
55

56 **2,6-Bis((trimethylsilyl)ethynyl)-9,10-dimethoxyanthracene (4a)**

57
58 To a suspension of **3a** (200 mg, 0.50 mmol, 1 eq), $\text{Pd}(\text{PPh}_3)_4$ (58 mg, 0.05 mmol, 0.1
59
60

1
2
3
4 eq) and CuI (19 mg, 0.10 mmol, 0.2 eq) in 10 mL of diisopropylamine (dried over molecular
5
6 sieve 4Å) and 10 mL of THF was added trimethylsilylacetylene (0.28 mL, 2 mmol, 4 eq)
7
8 under a nitrogen atmosphere at room temperature. The mixture was heated to 80 °C and
9
10 stirred overnight. After cooled to room temperature, the mixture was filtered through a short
11
12 pad of celite, and the filtrate was concentrated under reduced pressure. The residue was
13
14 purified by column chromatography using hexane/CH₂Cl₂ (4/1, v/v) as the eluent, yielding
15
16 190 mg (0.44 mmol, 88%) of **4a** as a yellow solid. m.p.: 232–234 °C. ¹H-NMR (400 MHz,
17
18 CDCl₃): δ = 8.40 (s, 2H), 8.20 (d, ³J(H, H) = 9.2 Hz, 2H), 7.49 (dd, ³J(H, H) = 8.8 Hz, ⁴J(H,
19
20 H) = 1.6 Hz, 2H), 4.09 (s, 6H), 0.31(s, 18H) ppm; ¹³C{¹H}-NMR (100 MHz, CDCl₃): δ =
21
22 144.8, 128.2, 127.1, 125.2, 124.4, 122.9, 120.5, 105.8, 95.9, 63.8, 0.2 ppm; HRMS-ESI⁺
23
24 (m/z): calcd. for C₂₆H₃₀O₂Si₂ [M]⁺ 430.1778; found, 430.1778.

2,6-Bis((trifluoromethyl)ethynyl)-9,10-dimethoxyanthracene (**5a**)

35
36 To a test tube equipped with a magnetic stir bar was added **4a** (172 mg, 0.4 mmol, 1
37
38 eq), 8 mL DMF, TMEDA (360 μL, 2.4 mmol, 6 eq.) and a 0.5 M solution (4.8 mL, 6 eq.) of
39
40 CuCF₃ in DMF, which was prepared from CHF₃ and CuCl following the reported procedure
41
42 (Method B).¹⁵ The reaction mixture was stirred in air at room temperature for 18 h, then
43
44 diluted with diethyl ether (5 mL) and poured into 250 mL ice water. After stirring for 30 min,
45
46 the mixture was filtered and the solid was washed with water. The crude product was purified
47
48 by column chromatography using hexane/CH₂Cl₂ (4/1, v/v) as the eluent, yielding 100 mg
49
50 (0.24 mmol, 59%) of **5a** as a yellow solid. m.p.: 249–250 °C. ¹H-NMR (400 MHz, CDCl₃): δ
51
52 = 8.59 (s, 2H), 8.32 (d, ³J(H, H) = 9.2 Hz, 2H), 7.56 (dd, ³J(H, H) = 8.8 Hz, ⁴J(H, H) = 1.2
53
54 Hz, 2H), 4.14 (s, 6H) ppm; ¹³C{¹H}-NMR was not recorded due to its low solubility;
55
56
57
58
59
60

¹⁹F-NMR (376 MHz, CDCl₃): δ = -50.7 (s, 3F) ppm; HRMS-ESI⁺ (*m/z*): calcd. for C₂₂H₁₂F₆O₂ [M]⁺ 422.0736; found, 422.0737.

2,6-Bis((trifluoromethyl)ethynyl)-9,10-anthraquinone (1a)

To a stirred solution of **5a** (50 mg, 0.12 mmol, 1 eq) in anhydrous THF (40 mL) was added an aqueous solution (3 mL) of NBS (428 mg, 2.4 mmol, 20 eq) under a nitrogen atmosphere at room temperature. The mixture was stirred at room temperature for 30 min and then extracted with diethyl ether. The combined organic layers were washed with water and brine, dried over anhydrous Na₂SO₄, and concentrated under reduced pressure to give almost pure product. Further purification by recrystallization from acetone gave 45 mg (0.11 mmol, 95%) of **1a** as a yellow solid. m.p.: 188–190 °C. ¹H-NMR (400 MHz, CDCl₃): δ = 8.52 (d, ⁴*J*(H, H) = 1.6 Hz, 2H), 8.39 (d, ³*J*(H, H) = 8 Hz, 2H), 8.0 (dd, ³*J*(H, H) = 8 Hz, ⁴*J*(H, H) = 1.6 Hz, 2H) ppm; ¹³C{¹H}-NMR was not recorded due to its low solubility; ¹⁹F-NMR (376 MHz, CDCl₃): δ = -51.5 (s, 3F) ppm. HRMS-ESI⁺ (*m/z*): calcd. for C₂₀H₆F₆O₂ [M]⁺ 392.0267; found, 392.0271.

2,7-Dibromo-9,10-dimethoxyanthracene (3b)

2,7-Dibromo-9,10-anthraquinone (**2b**)²⁰ (250 mg, 0.68 mmol, 1 eq) and tetrabutylammonium bromide (219 mg, 0.68 mmol, 1 eq) were dissolved in 20 mL of CH₂Cl₂. To this solution was added a solution of Na₂S₂O₄ (268 mg, 1.54 mmol, 2.25 eq) and 1g of NaOH in 5 mL of water under an atmosphere of N₂, and the resulting mixture was stirred for 2 h at room temperature. After slow addition of methyl iodide (0.42 mL, 6.8 mmol, 10 eq) via a syringe, the mixture was stirred at room temperature under an atmosphere of N₂ for another 8 h and then extracted with CH₂Cl₂. The combined organic layers were washed with water and brine, dried over anhydrous Na₂SO₄, and concentrated under reduced pressure. The

product was purified by column chromatography using hexane/CH₂Cl₂ (4/1, v/v) as the eluent, yielding 147 mg (0.37 mmol, 54%) of **3b** as a yellow solid. m.p.: 207–208 °C. ¹H-NMR (400 MHz, CDCl₃): δ = 8.44 (d, ⁴J(H, H) = 1.6 Hz, 2H), 8.15 (d, ³J(H, H) = 9.2 Hz, 2H), 7.56 (dd, ³J(H, H) = 9.2 Hz, ⁴J(H, H) = 2 Hz, 2H), 4.10 (s, 3H), 4.09 (s, 3H) ppm; ¹³C{¹H}-NMR (100 MHz, CDCl₃): δ = 149.4, 146.8, 129.4, 126.5, 124.8, 124.8, 123.5, 121.0, 63.8, 63.7 ppm; HRMS-ESI⁺ (*m/z*): calcd. for C₁₆H₁₂Br₂O₂ [M]⁺ 395.9178; found, 395.9172.

2,7-Bis((trimethylsilyl)ethynyl)-9,10-dimethoxyanthracene (**4b**)

To a suspension of **3b** (120 mg, 0.3 mmol, 1 eq), Pd(PPh₃)₄ (35 mg, 0.03 mmol, 0.1 eq) and CuI (11 mg, 0.06 mmol, 0.2 eq) in 6 mL of diisopropylamine (dried over molecular sieve 4Å) and 6 mL of THF was added trimethylsilylacetylene (0.18 mL, 1.2 mmol, 4 eq) under a nitrogen atmosphere at room temperature. The mixture was kept under the nitrogen atmosphere and stirred at 80 °C overnight, then cooled to room temperature, and filtered through a short pad of celite. The filtrate was concentrated under reduced pressure. The residue was purified by column chromatography using hexane/CH₂Cl₂ (4/1, v/v) as the eluent, yielding 120 mg (0.28 mmol, 93%) of **4b** as a yellow solid. m.p.: 193–194 °C. ¹H-NMR (400 MHz, CDCl₃): δ = 8.42 (s, 2H), 8.20 (d, ³J(H, H) = 9 Hz, 2H), 7.50 (d, ³J(H, H) = 8.9 Hz, 2H), 4.13 (s, 3H), 4.08 (s, 3H), 0.31 (s, 18H) ppm; ¹³C{¹H}-NMR (100 MHz, CDCl₃): δ = 148.5, 148.4, 128.2, 127.1, 124.8, 124.6, 122.8, 120.2, 105.6, 95.6, 63.9, 63.4, 0.02 ppm; HRMS-ESI⁺ (*m/z*): calcd. for C₂₆H₃₀O₂Si₂ [M]⁺ 430.1779; found, 430.1778.

2,7-Bis((trifluoromethyl)ethynyl)-9,10-dimethoxyanthracene (**5b**)

To a test tube equipped with a magnetic stir bar was added **4b** (86 mg, 0.2 mmol, 1 eq), 4 mL DMF, TMEDA (180 μL, 1.2 mmol, 6 eq) and a 0.5 M solution (2.4 mL, 6 eq.) of CuCF₃ in DMF, which was prepared from CHF₃ and CuCl following the reported procedure (Method B).¹⁵ The mixture was stirred in air at room temperature for 18 h, then diluted with diethyl ether (2 mL) and poured into 100 mL of ice water. After stirring for 30 min, the

1
2
3 mixture was filtered and the solid was washed with water. The crude product was purified by
4 column chromatography using hexane/CH₂Cl₂ (4/1, v/v) as the eluent, yielding 35 mg (0.083
5 mmol, 42%) of **5b** as a yellow solid. m.p.: 209–210 °C. ¹H-NMR (400 MHz, CDCl₃): δ =
6 8.58 (s, 2H), 8.31 (d, ³J(H, H) = 8.8 Hz, 2H), 7.56 (dd, ³J(H, H) = 9.2 Hz, ⁴J(H, H) = 1.6 Hz,
7 2H), 4.16 (s, 3H), 4.11 (s, 3H) ppm; ¹³C{¹H}-NMR (100 MHz, CDCl₃): δ = 149.8, 148.9,
8 129.6, 127.5, 126.0, 124.7, 123.7, 118.8 (q, *J*_{CF} = 255.1 Hz), 116.2, 86.9 (q, *J*_{CF} = 6.2 Hz),
9 77.4 (q, *J*_{CF} = 52.8 Hz), 64.6, 63.8 ppm; ¹⁹F-NMR (376 MHz, CDCl₃): δ = –51.0 (s, 3F) ppm.
10
11
12
13
14
15
16
17
18
19
20
21
22 HRMS-ESI⁺ (*m/z*): calcd. for C₂₂H₁₂F₆O₂ [M]⁺ 422.0736; found, 422.0739.

2,7-Bis((trifluoromethyl)ethynyl)-9,10-anthraquinone (**1b**)

23
24 To a stirred solution of **5b** (35 mg, 0.081 mmol, 1 eq) in anhydrous THF (40 mL) was
25 added an aqueous solution (2 mL) of (NH₄)₂Ce(NO₃)₆ (132 mg, 0.24 mmol, 3 eq.) under a
26 nitrogen atmosphere at 0 °C. The mixture was allowed to warm slowly to room temperature
27 and stirred for 30 min. Extracted with diethyl ether, and then the combined organic layers
28 were washed with water and brine, dried over anhydrous Na₂SO₄, and concentrated under
29 reduced pressure to give almost pure product. Further purification was preceded by
30 recrystallization with acetone to give 30 mg (0.076 mmol, 94%) of **1b** as a yellow solid. m.p.:
31 207–208 °C. ¹H-NMR (400 MHz, CDCl₃): δ = 8.53 (d, ⁴J(H, H) = 1.2 Hz, 2H), 8.38 (d, ³J(H,
32 H) = 8 Hz, 2H), 8.0 (dd, ³J(H, H) = 8 Hz, ⁴J(H, H) = 1.6 Hz, 2H) ppm; ¹³C{¹H}-NMR was
33 not recorded due to its low solubility; ¹⁹F-NMR (376 MHz, CDCl₃): δ = –51.5 (s, 3F) ppm.
34
35
36
37
38
39
40
41
42
43
44
45
46
47
48
49 FTICR MS (*m/z*): calcd. for C₂₀H₇O₂F₆ [M+H]⁺ 393.0345; found, 393.0343.

2,3-Dibromo-9,10-anthraquinone (**2c**)

50
51 To a stirred solution of 500 mg (2.1 mmol, 1.2 eq) of 3,4-dibromothiophene (**8**) and
52 277 mg (1.75 mmol, 1eq) of 1,4-naphthoquinone (**9**) in CHCl₃ (10 mL) at 75 °C was added
53 m-CPBA (70w%, 2.4 g, 9.73 mmol, 5.56 eq) in small portions. After 48 h, the mixture was
54 cooled and poured into a saturated aqueous solution of Na₂CO₃. After the mixture was stirred
55
56
57
58
59
60

1
2
3 for 15 min at room temperature, it was extracted with CH₂Cl₂. The combined organic layers
4
5 were washed with water and brine, dried over anhydrous Na₂SO₄, and concentrated under
6
7 reduced pressure. The residue was washed with EtOH to give 354 mg (0.97 mmol, 55%) of
8
9 **2c** as a brown solid. ¹H-NMR (400 MHz, CDCl₃): δ = 8.53 (s, 2H), 8.33(dd, ³J(H, H) = 5.6
10
11 Hz, ⁴J(H, H) = 3.2 Hz, 2H), 7.86 (dd, ³J(H, H) = 6 Hz, ⁴J(H, H) = 3.6 Hz, 2H) ppm. The ¹H
12
13 NMR data are consistent with the reported.²¹
14
15

16 17 **2,3-Dibromo-9,10-dimethoxyanthracene (3c)**

18
19 300 mg (0.82 mmol, 1 eq) of 2,3-dibromo-9,10-anthraquinone (**2c**) and
20
21 tetrabutylammonium bromide (264 mg, 0.82 mmol, 1 eq.) were dissolved in 60 mL of
22
23 CH₂Cl₂. To this solution was added a solution of Na₂S₂O₄ (321 mg, 1.84 mmol, 2.25 eq) and
24
25 1.8 g NaOH in 9 mL of water under an atmosphere of N₂, and the resulting mixture was
26
27 stirred for 2 h at room temperature. After slow addition of methyl iodide (0.52 mL, 8.2 mmol,
28
29 10 eq) via a syringe, the mixture was stirred at room temperature under an atmosphere of N₂
30
31 for another 8 h and then extracted with CH₂Cl₂. The combined organic layers were washed
32
33 with water and brine, dried over anhydrous Na₂SO₄, and concentrated under reduced pressure.
34
35 The product was purified by column chromatography using hexane/CH₂Cl₂ (4/1, v/v) as the
36
37 eluent, yielding 112 mg (0.26 mmol, 32 %) of **3c** as a yellow solid. m.p.: 173–175 °C.
38
39 ¹H-NMR (400 MHz, CDCl₃): δ = 8.59 (s, 2H), 8.28 (dd, ³J(H, H) = 6.8 Hz, ⁴J(H, H) = 3.2 Hz,
40
41 2H), 7.55 (dd, ³J(H, H) = 6.8 Hz, ⁴J(H, H) = 3.6 Hz, 2H), 4.11 (s, 6H) ppm; ¹³C {¹H}-NMR
42
43 (100 MHz, CDCl₃): δ = 147.9, 127.4, 126.4, 125.9, 124.3, 122.8, 122.2, 63.8 ppm;
44
45 HRMS-ESI⁺ (*m/z*): calcd. for C₁₆H₁₂Br₂O₂ [M]⁺ 395.9178; found, 395.9184.
46
47
48
49

50 51 **2,3-Bis((trimethylsilyl)ethynyl)-9,10-dimethoxyanthracene (4c)**

52
53 To a suspension of **3c** (100 mg, 0.25 mmol, 1 eq), Pd(PPh₃)₄ (29 mg, 0.025 mmol, 0.1
54
55 eq) and CuI (9.5 mg, 0.05 mmol, 0.2 eq) in 5 mL of dry diisopropylamine and 5 mL of THF
56
57 was added trimethylsilylacetylene (0.15 mL, 1 mmol, 4 eq) under a nitrogen atmosphere at
58
59
60

1
2
3 room temperature. The mixture was heated to 80 °C and stirred overnight. After cooled to
4 room temperature, was filtered through a short pad of celite, and the filtrate was concentrated
5 under reduced pressure. The residue was purified by column chromatography using hexane/
6 CH₂Cl₂ (4:1) as the eluent, yielding 73 mg (0.17 mmol, 68%) of **4c** as a yellow solid. m.p.:
7 218–219 °C. ¹H-NMR (400 MHz, CDCl₃): δ = 8.44 (s, 2H), 8.27 (dd, ³J(H, H) = 6.8 Hz, ⁴J(H,
8 H) = 3.2 Hz, 2H), 7.52 (dd, ³J(H, H) = 6.8 Hz, ⁴J(H, H) = 3.6 Hz, 2H), 4.11 (s, 6H), 0.33 (s,
9 18H) ppm; ¹³C{¹H}-NMR (100 MHz, CDCl₃): δ = 148.5, 127.9, 126.3, 126.2, 123.3, 123.0,
10 121.2, 104.0, 98.4, 63.8, 0.3 ppm; HRMS-ESI⁺ (*m/z*): calcd. for C₂₆H₃₀O₂Si₂Na [M+Na]⁺
11 453.1676; found, 453.1677.

2,3-Bis((trifluoromethyl)ethynyl)-9,10-dimethoxyanthracene (**5c**)

24
25 To a test tube equipped with a magnetic stir bar was added **4c** (64 mg, 0.15 mmol, 1
26 eq), 3 mL DMF, TMEDA (135 μL, 0.9 mmol, 6 eq) and a 0.5 M solution (1.8 mL, 6 eq.) of
27 CuCF₃ in DMF, which was prepared from CHF₃ and CuCl following the reported procedure
28 (Method B).¹⁵ The reaction mixture was stirred in air at room temperature for 18 h, then
29 diluted with diethyl ether (2 mL) and poured into 100 mL ice water. After stirring for 30 min,
30 the mixture was filtered and the solid was washed with water. The crude product was purified
31 by column chromatography using hexane/CH₂Cl₂ (4/1, v/v) as the eluent, yielding 35 mg
32 (0.083 mmol, 56 %) of **5c** as a yellow solid. m.p.: 251–252 °C. ¹H-NMR (400 MHz, CDCl₃):
33 δ = 8.62 (s, 2H), 8.34 (dd, ³J(H, H) = 6.8 Hz, ⁴J(H, H) = 3.2 Hz, 2H), 7.64 (dd, ³J(H, H) = 6.8
34 Hz, ⁴J(H, H) = 3.2 Hz, 2H), 4.14 (s, 6H) ppm; ¹³C{¹H}-NMR (100 MHz, CDCl₃): δ = 149.5,
35 130.5, 127.5, 127.4, 123.2, 123.0, 118.7 (q, *J*_{CF} = 255.8 Hz), 115.8, 84.4 (q, *J*_{CF} = 6.6 Hz),
36 80.4 (q, *J*_{CF} = 52.8 Hz), 64.2 ppm; ¹⁹F-NMR (376 MHz, CDCl₃): δ = -51.2 (s, 3F) ppm.
37 HRMS-ESI⁺ (*m/z*): calcd. for C₂₂H₁₂F₆O₂ [M]⁺ 422.0736; found, 422.0731.

2,3-Bis((trifluoromethyl)ethynyl)-9,10-anthraquinone (**1c**)

56 To a stirred solution of **5c** (34 mg, 0.08 mmol, 1 eq) in dry THF (40 mL) was added
57
58
59
60

1
2
3 an aqueous solution (2 mL) of $(\text{NH}_4)_2\text{Ce}(\text{NO}_3)_6$ (132 mg, 0.24 mmol, 3 eq) under a nitrogen
4 atmosphere at 0 °C. The mixture was allowed to warm slowly to room temperature and
5
6 stirred for 30 min. Extracted with diethyl ether, and then the combined organic layers were
7
8 washed with water and brine, dried over anhydrous Na_2SO_4 , and concentrated under reduced
9
10 pressure to give almost pure product. Further purification was preceded by recrystallization
11
12 with acetone to give 30 mg (0.077 mmol, 96%) of **1c** as a yellow solid. m.p.: 173–174 °C.
13
14 $^1\text{H-NMR}$ (400 MHz, CDCl_3): δ = 8.56 (s, 2H), 8.36 (dd, $^3J(\text{H}, \text{H}) = 5.6$ Hz, $^4J(\text{H}, \text{H}) = 3.2$ Hz,
15
16 2H), 7.90 (dd, $^3J(\text{H}, \text{H}) = 5.6$ Hz, $^4J(\text{H}, \text{H}) = 3.2$ Hz, 2H) ppm; $^{13}\text{C}\{^1\text{H}\}$ -NMR was not
17
18 recorded due to its low solubility; $^{19}\text{F-NMR}$ (376 MHz, CDCl_3): δ = -51.5 (s, 3F) ppm.
19
20 FTICR MS (m/z): calcd. for $\text{C}_{20}\text{H}_7\text{O}_2\text{F}_6$ $[\text{M}+\text{H}]^+$ 393.0345; found, 393.0343.
21
22
23
24
25

26 **1,5-Dichloro-9,10-dimethoxyanthracene (3d)**

27
28 1 g (3.6 mmol, 1 eq) of 1,5-dichloro-9,10-anthraquinone (**2d**) and
29
30 tetrabutylammonium bromide (1.16 g, 3.6 mmol, 1 eq) were dissolved in 140 mL CH_2Cl_2 .
31
32 $\text{Na}_2\text{S}_2\text{O}_4$ (1.4 g, 8.12 mmol, 2.25 eq) dissolved in 5 M NaOH (8 g NaOH in 40 mL water)
33
34 was added under an atmosphere of N_2 and the mixture was stirred for 2 h at room temperature.
35
36 After slow addition of methyl iodide (2.3 mL, 36 mmol, 10 eq) via a syringe, the mixture was
37
38 stirred at room temperature under an atmosphere of N_2 for another 8 h and then extracted with
39
40 CH_2Cl_2 . The combined organic layers were washed with water and brine, dried over
41
42 anhydrous Na_2SO_4 , and concentrated under reduced pressure. The product was purified by
43
44 column chromatography using hexane/ CH_2Cl_2 (4/1, v/v) as the eluent, yielding 430 mg (1.4
45
46 mmol, 39 %) of **3d** as a yellow solid. m.p.: 197–198 °C. $^1\text{H-NMR}$ (400 MHz, CDCl_3): δ =
47
48 8.36 (d, $^3J(\text{H}, \text{H}) = 8.8$ Hz, 2H), 7.60 (d, $^3J(\text{H}, \text{H}) = 7.2$ Hz, 2H), 7.40 (dd, $^3J(\text{H}, \text{H}) = 8.8$ Hz,
49
50 $^3J(\text{H}, \text{H}) = 7.2$ Hz, 2H), 4.00 (s, 6H) ppm; $^{13}\text{C}\{^1\text{H}\}$ -NMR (100 MHz, CDCl_3): δ = 149.1,
51
52 129.6, 129.0, 128.9, 125.4, 122.7, 122.5, 64.3 ppm; HRMS-ESI⁺ (m/z): calcd. for
53
54 $\text{C}_{16}\text{H}_{12}\text{Cl}_2\text{O}_2$ $[\text{M}]^+$ 306.0209; found, 306.0205.
55
56
57
58
59
60

1,5-Bis((trimethylsilyl)ethynyl)-9,10-dimethoxyanthracene (4d)

Isopropylmagnesium chloride (2 M in THF, 6.5 mL, 13 mmol, 10 eq) and trimethylsilylacetylene (1.84 mL, 13 mmol, 10 eq) were dissolved in 20 mL dry THF and heated for 2 h at 60 °C. The resulting solution of [(trimethylsilyl)ethynyl]magnesium bromide was added dropwise into a stirred solution of **3d** (400 mg, 1.3 mmol, 1 eq), triphenylphosphine (24 mg, 0.09 mmol, 0.07 eq), and [Ni(acac)₂] (23 mg, 0.09 mmol, 0.07 eq) in 40 mL anhydrous THF. The mixture was refluxed for 16 h under a nitrogen atmosphere. After cooling, the mixture was quenched with NH₄Cl aqueous, extracted with diethyl ether. Then the combined organic layers were washed with water and brine, dried over anhydrous Na₂SO₄, and concentrated under reduced pressure. The crude product was purified column chromatography using hexane/ CH₂Cl₂ (4/1, v/v) as the eluent, yielding 438 mg (1.01 mmol, 78%) of **4d** as a yellow solid. m.p.: 207–208 °C. ¹H-NMR (400 MHz, CDCl₃): δ = 8.37 (dd, ³J(H, H) = 8.8 Hz, ⁴J(H, H) = 0.8 Hz, 2H), 7.81 (dd, ³J(H, H) = 6.8 Hz, ⁴J(H, H) = 0.8 Hz, 2H), 7.44 (dd, ³J(H, H) = 6.8 Hz, ³J(H, H) = 8.8 Hz, 2H), 4.04 (s, 6H), 0.35 (s, 18H) ppm; ¹³C{¹H}-NMR (100 MHz, CDCl₃): δ = 149.6, 135.5, 126.6, 124.9, 124.5, 124.3, 117.8, 106.8, 97.2, 64.4, 0.3 ppm; HRMS-ESI⁺ (*m/z*): calcd. for C₂₆H₃₀O₂Si₂ [M]⁺ 430.1779; found, 430.1774; calcd. for C₂₆H₃₀O₂Si₂Na [M+Na]⁺ 453.1676; found, 453.1671.

1,5-Bis((trifluoromethyl)ethynyl)-9,10-dimethoxyanthracene (5d)

To a test tube equipped with a magnetic stir bar was added **4d** (172 mg, 0.4 mmol, 1 eq), 8 mL DMF, TMEDA (360 μL, 0.9 mmol, 6 eq) and a 0.5 M solution (4.8 mL, 6 eq.) of CuCF₃ in DMF, which was prepared from CHF₃ and CuCl following the reported procedure (Method B).¹⁵ The reaction mixture was stirred in air at room temperature for 18 h, then diluted with diethyl ether (5 mL) and poured into 250 mL ice water. After stirring for 30 min, the mixture was filtered and the solid was washed with water. The crude product was purified by column chromatography using hexane/CH₂Cl₂ (4/1, v/v) as the eluent, yielding 58 mg

(0.14 mmol, 34 %) of **5d** as a yellow solid. m.p.: 148–149 °C. ¹H-NMR (400 MHz, CDCl₃): δ = 8.50 (d, ³J(H, H) = 8.8 Hz, 2H), 7.94 (d, ³J(H, H) = 6.4 Hz, 2H), 7.56 (dd, ³J(H, H) = 6.8 Hz, ³J(H, H) = 8.8 Hz, 2H), 4.07 (s, 6H) ppm; ¹³C{¹H}-NMR (100 MHz, CDCl₃): δ = 149.6, 137.0, 126.7, 126.5, 125.3, 124.4, 119.3 (q, J_{CF} = 254.7 Hz), 113.4, 88.6 (q, J_{CF} = 6.9 Hz), 79.0 (q, J_{CF} = 51.8 Hz), 64.4 ppm; ¹⁹F-NMR (376 MHz, CDCl₃): δ = -50.3 (s, 3F) ppm. HRMS-ESI⁺ (m/z): calcd. for C₂₂H₁₂F₆O₂ [M]⁺ 422.0736; found, 422.0729.

1,5-Bis((trifluoromethyl)ethynyl)-9,10-anthraquinone (**1d**)

To a stirred solution of **5d** (42 mg, 0.1 mmol, 1 eq) in dry THF (40 mL) was added an aqueous solution (5 mL) of (NH₄)₂Ce(NO₃)₆ (164 mg, 0.3 mmol, 3 eq) under a nitrogen atmosphere at 0 °C. The mixture was allowed to warm slowly to room temperature and stirred for 30 min, then extracted with diethyl ether. The combined organic layers were washed with water and brine, dried over MgSO₄, and concentrated under reduced pressure to give almost pure product. Further purification was preceded by recrystallization with acetone to give 38 mg (0.097 mmol, 97%) of **1d** as a yellow solid. m.p.: 195–196 °C. ¹H-NMR (400 MHz, CDCl₃): δ = 8.53 (dd, ³J(H, H) = 8 Hz, ⁴J(H, H) = 1.2 Hz, 2H), 8.04 (d, ³J(H, H) = 7.6 Hz, ⁴J(H, H) = 1.2 Hz, 2H), 7.89 (t, ³J(H, H) = 8 Hz, 2H) ppm; ¹³C{¹H}-NMR was not recorded due to its low solubility; ¹⁹F-NMR (376 MHz, CDCl₃): δ = -51.2 (s, 3F) ppm. FTICR MS (m/z): calcd. for C₂₀H₇O₂F₆ [M+H]⁺ 393.0345; found, 393.0343.

Cyclic voltammetry. Cyclic voltammetry was performed on a PAR Potentiostat/Galvanostat Model 263A Electrochemical Station (Princeton Applied Research) at a scan rate of 30 mVs⁻¹. All compounds were dissolved in anhydrous CH₂Cl₂ that contained 0.1 M of tetrabutylammonium hexafluorophosphate (Bu₄NPF₆) as the supporting electrolyte. A platinum bead was used as a working electrode, a platinum wire was used as an auxiliary

1
2
3
4 electrode, and a silver wire was used as a pseudo-reference. Ferrocenium/ferrocene (Fc^+/Fc)
5
6 was used as an internal standard.
7

8
9 **UV-vis absorption spectra.** UV-vis absorption spectra were recorded on a Shimadzu
10
11 UV-3600 Plus UV-VIS-NIR spectrophotometer.
12

13
14 **Crystal Structure Determination.** The single crystals were grown by diffusion of ethyl
15
16 acetate vapor into a solution of chloroform. X-ray crystallography data were collected on a
17
18 Bruker AXS Kappa ApexII Duo Diffractometer or Bruker D8 Venture Diffractometer.
19

20
21 **DFT calculations.** The frontier molecular orbitals were calculated using the Gaussian 09W
22
23 software package. The geometries were optimized at the B3LYP level of DFT with the
24
25 6-31G(d,p) basis set, and the molecular orbitals were then calculated with the 6-311++G(d, p)
26
27 basis set.
28
29
30

31 32 **Fabrication and characterization of organic field effect transistors (OFETs)** 33

34
35 To fabricate OFETs, the dielectric layer was first formed following the reported
36
37 method.⁴ A solution of $\text{Al}(\text{NO}_3)_3 \cdot 9\text{H}_2\text{O}$ in ethanol (0.15 mol/L) was first spin-cast onto a
38
39 highly doped silicon substrate, which had a 100 nm-thick layer of SiO_2 on its top. The
40
41 spin-cast film was then baked at 300 °C for 30 minutes to form a thin layer of aluminum
42
43 oxide (Al_2O_3). To modify the Al_2O_3 layer with a self-assembled monolayer (SAM) of
44
45 12-cyclohexyldodecylphosphonic acid (CDPA),¹⁸ the Al_2O_3 -coated SiO_2/Si wafer was soaked
46
47 in a 0.3 mM solution of CDPA in isopropanol at room temperature for 12 hours, then rinsed
48
49 with isopropanol and dried with a flow of nitrogen. The capacitance per unit area (C_i) of
50
51 CDPA- $\text{Al}_2\text{O}_3/\text{SiO}_2$ was measured from a metal-insulator-metal structure, where
52
53 vacuum-deposited gold (0.2 mm×1 mm) was the top electrode and the highly doped silicon
54
55
56
57
58
59
60

1
2
3
4 substrate was the bottom electrode, with the frequency ranging from 100 Hz to 100 kHz. As
5
6 taken at the lowest frequency (100 Hz), the C_i of CDPA- $\text{Al}_2\text{O}_3/\text{SiO}_2$ is $26 \pm 1 \text{ nF/cm}^2$.
7
8

9
10 Thin films of **1a**, **1b** were dip-coated on the CDPA- $\text{Al}_2\text{O}_3/\text{SiO}_2$ dielectric by
11
12 immersing the substrate (substrate size: 1.2 cm \times 0.6 cm) vertically in a solution and then
13
14 pulling up at a constant speed with a LongerPump TJ-3A syringe pump. The optimized
15
16 conditions for dip coating are: **1a** in $\text{CH}_2\text{Cl}_2/\text{acetone}(3/1, \text{ v/v, saturated})$ with a pulling speed
17
18 of 250 $\mu\text{m/min}$; **1b** in $\text{CH}_2\text{Cl}_2/\text{acetone} (1/1, \text{ v/v, } 2 \text{ mg/mL})$ with a pulling speed of 200
19
20 $\mu\text{m/min}$. Thin films of **1c**, **1d** were drop-cast on the CDPA- $\text{Al}_2\text{O}_3/\text{SiO}_2$ dielectric by drop a
21
22 solution onto a tilted substrate (three drops, tilt angle = $\sim 5^\circ$), which was covered with a glass
23
24 dish to allow the solvent to evaporate slowly. The optimized concentrations and solvents are
25
26 0.5 mg/mL of **1c** in CHCl_3 and 1.0 mg/mL of **1d** in $\text{CH}_2\text{Cl}_2/\text{acetone} (2/1, \text{ v/v})$. Top contact
27
28 drain and source gold electrodes were then vacuum-deposited through a shadow mask onto
29
30 the organic films using an Edwards Auto 306 vacuum coating system with a Turbomolecular
31
32 pump at a pressure of 4.0×10^{-6} torr or lower, with a deposition rate of ca. 2 nm/min to the
33
34 desired thickness as measured by a quartz crystal sensor.
35
36
37
38
39
40
41
42

43
44 The current-voltage measurement was carried out on a JANIS ST-500-20-4TX probe
45
46 station with a Keithley 4200 Semiconductor Characterization System at room temperature
47
48 under vacuum (background pressure of 2.0×10^{-4} mbar or lower). The field effect mobility
49
50 was extracted from transfer I-V curve using the equation: $I_D = (\mu WC_i/2L) (V_{GS} - V_{th})^2$, where
51
52 I_D is the drain current, μ is field effect mobility, W and L are the effective channel width and
53
54 length, respectively, C_i is the capacitance per unit area for the CDPA- $\text{Al}_2\text{O}_3/\text{SiO}_2$ substrates,
55
56 V_{GS} and V_{th} are the gate and threshold voltage, respectively. The average field effect mobility
57
58
59
60

1
2
3
4 for each compound was obtained from at least 30 channels on more than 6 individual
5
6 substrates.
7

8
9 Polarized optical images of the devices were obtained using a Nikon 50IPOL
10
11 microscope. The AFM images were collected with a Nanoscope IIIa Multimode Microscope
12
13 (Digital Instruments) using tapping mode and in air under ambient conditions. X-ray
14
15 diffraction from thin films were recorded on a SmartLab X-Ray Refractometer.
16
17

18 19 **Supporting Information**

20
21
22 Cyclic voltammograms, UV-vis absorption spectra, DFT calculation data,
23
24 characterization of thin films and field effect transistors of **1a–d** and NMR spectra for all
25
26 compounds. Crystallographic data for compound **1a**, **1c**, **1d**.
27
28

29 30 **Acknowledgements**

31
32 We thank Ms. Hoi Shan Chan (the Chinese University of Hong Kong) for the single
33
34 crystal crystallography. Ms. Zhao thanks the Hong Kong PhD Fellowship for financial
35
36 support, and G. C. Tusi thanks the Research Grants Council of Hong Kong (CUHK
37
38 24301217), the Chinese University of Hong Kong (the Faculty Strategic Fund for Research
39
40 from the Faculty of Science and the Direct Grant for Research) and the Key Laboratory of
41
42 Organofluorine Chemistry, Shanghai Institute of Organic Chemistry, Chinese Academy of
43
44 Science for research funding.
45
46
47
48
49
50

51 52 53 **Reference**

- 54
55
56
57 1 a) Voss, D. Cheap and cheerful circuits. *Nature* **2000**, *407*, 442–444. b) Mabeck, J. T.;
58
59 Malliaras, G. G. Chemical and biological sensors based on organic thin-film transistors.
60

- 1
2
3
4 *Anal. Bioanal. Chem.* **2006**, *384*, 343–353. c) Someya, T.; Dodabalapur, A.; Huang, J.;
5
6 See, K. C.; Katz, H. E. Chemical and physical sensing by organic field-effect
7
8 transistors and related devices. *Adv. Mater.* **2010**, *22*, 3799–3811. d) Gelinck, G.;
9
10 Heremans, P.; Nomoto, K.; Anthopoulos, T. Organic transistors in optical displays and
11
12 microelectronic applications. *Adv. Mater.* **2010**, *22*, 3778–3798. e) Lee, Y. H.; Jang, M.;
13
14 Lee, M. Y.; Kweon, O. Y.; Oh, J. H. Flexible field-effect transistor-type sensors based
15
16 on conjugated molecules. *Chem* **2017**, *3*, 724–763.
17
18
19
20
21 2 a) Shukla, D.; Nelson, S. F.; Freeman, D. C.; Rajeswaran, M.; Ahearn, W. G.; Meyer,
22
23 D. M.; Carey, J. T. Thin-Film Morphology Control in Naphthalene-Diimide-Based
24
25 Semiconductors: High Mobility n-Type Semiconductor for Organic Thin-Film
26
27 Transistors. *Chem. Mater.* **2008**, *20*, 7486–7491. b) Wu, H.; Wang, Y.; Qiao, X.; Wang,
28
29 D.; Yang, X., Li, H. Pyrrolo [3, 2-b] pyrrole-Based Quinoidal Compounds For High
30
31 Performance n-Channel Organic Field-Effect Transistor. *Chem. Mater.* **2018**, *30*,
32
33 6992–6997. c) Zhu, C.; Zhao, Z.; Chen, H.; Zheng, L.; Li, X.; Chen, J.; Sun, Y.; Liu, F.;
34
35 Guo, Y.; Liu, Y. Regioregular bis-pyridal[2,1,3] thiadiazole-based semiconducting
36
37 polymer for high-performance ambipolar transistors. *J. Am. Chem. Soc.* **2017**, *139*,
38
39 17735–17738. d) Zhao, Z.; Yin, Z.; Chen, H.; Zheng, L.; Zhu, C.; Zhang, L.; Tan, S.;
40
41 Wang, H.; Guo, Y.; Tang, Q.; Liu, Y. High-performance, air-stable field-effect
42
43 transistors based on heteroatomsubstituted naphthalenediimidebenzothiadiazole
44
45 copolymers exhibiting ultrahigh electron mobility up to $8.5 \text{ cm}^2 \text{ V}^{-1} \text{ s}^{-1}$. *Adv. Mater.*
46
47 **2017**, *29*, 1602410.
48
49
50
51
52
53
54
55
56 3 a) Xiang, L.; Ying, J.; Wang, W.; Xie, W. High mobility n-channel organic field-effect
57
58 transistor based a tetratetracontane interfacial layer on gate dielectrics. *IEEE Electron*
59
60

- 1
2
3
4 *Device Lett.* **2016**, *37*, 1632–1635. b) Li, H.; Tee, B. C.; Cha, J. J.; Cui, Y.; Chung, J.
5
6 W.; Lee, S. Y.; Bao, Z. High-mobility field-effect transistors from large-area
7
8 solution-grown aligned C₆₀ single crystals. *J. Am. Chem. Soc.* **2012**, *134*, 2760–2765. c)
9
10 Zheng, Y. Q.; Lei, T.; Dou, J. H.; Xia, X.; Wang, J. Y.; Liu, C. J.; Pei, J. Strong
11
12 Electron-Deficient Polymers Lead to High Electron Mobility in Air and Their
13
14 Morphology-Dependent Transport Behaviors. *Adv. Mater.* **2016**, *28*, 7213–7219. d)
15
16 Dou, J. H.; Zheng, Y. Q.; Yao, Z. F.; Yu, Z. A.; Lei, T.; Shen, X.; Luo, X. Y.; Sun, J.;
17
18 Zhang, S. D.; Ding, Y. F.; Han, G.; Yi, Y.; Wang, J. Y.; Pei, J. Fine-tuning of crystal
19
20 packing and charge transport properties of BDOPV derivatives through fluorine
21
22 substitution. *J. Am. Chem. Soc.* **2015**, *137*, 15947–15956.
23
24
25
26
27 4 Xu, X.; Yao, Y.; Shan, B.; Gu, X.; Liu, D.; Liu, J.; Xu, J.; Zhao, N.; Hu, W.; Miao, Q.
28
29 Electron Mobility Exceeding 10 cm² V⁻¹ s⁻¹ and Band-Like Charge Transport in
30
31 Solution-Processed n-Channel Organic Thin-Film Transistors. *Adv. Mater.* **2016**, *28*,
32
33 5276–5283.
34
35
36 5 Chu, M.; Fan, J. X.; Yang, S.; Liu, D.; Ng, C. F.; Dong, H.; Ren, A.; Miao, Q.
37
38 Halogenated Tetraazapentacenes with Electron Mobility as High as 27.8 cm² V⁻¹ s⁻¹ in
39
40 Solution-Processed n-Channel Organic Thin-Film Transistors. *Adv. Mater.* **2018**, *30*,
41
42 1803467.
43
44
45 6 Zhou, K.; Dong, H.; Zhang, H. L.; Hu, W. High performance n-type and ambipolar
46
47 small organic semiconductors for organic thin film transistors. *Phys. Chem. Chem.*
48
49 *Phys.* **2014**, *16*, 22448–22457.
50
51
52 7 Shan, B.; Miao, Q. Molecular design of n-type organic semiconductors for
53
54 high-performance thin film transistors. *Tetrahedron Lett.* **2017**, *58*, 1903–1911.
55
56
57 8 a) Tang, Q.; Liang, Z.; Liu, J.; Xu, J.; Miao, Q. N-heteroquinones: quadruple weak
58
59 hydrogen bonds and n-channel transistors. *Chem. Commun.* **2010**, *46*, 2977–2979. b)

- 1
2
3
4 Liang, Z.; Tang, Q.; Liu, J.; Li, J.; Yan, F.; Miao, Q. N-type organic semiconductors
5 based on π -deficient pentacenequinones: synthesis, electronic structures, molecular
6 packing, and thin film transistors. *Chem. Mater.* **2010**, *22*, 6438–6443. c) Shi, Z. F.;
7 Black, H. T.; Dadvand, A.; Perepichka, D. F. Pentacenobis (thiadiazole) dione, an
8 n-type semiconductor for field-effect transistors. *J. Org. Chem.* **2014**, *79*, 5858–5860.
- 9
10
11
12
13
14
15
16 9. Mamada, M.; Nishida, J.; Tokito, S.; Yamashita, Y. Anthraquinone derivatives
17 affording n-type organic thin film transistors. *Chem. Commun.* **2009**, 2177–2179.
- 18
19
20
21 10 Mamada, M.; Kumaki, D.; Nishida, J.; Tokito, S.; Yamashita, Y. Novel semiconducting
22 quinone for air-stable n-type organic field-effect transistors. *ACS Appl. Mater.*
23 *Interfaces.* **2010**, *2*, 1303–1307
- 24
25
26
27
28
29
30
31 11 a) Ando, S.; Nishida, J.; Tada, H.; Inoue, Y.; Tokito, S.; Yamashita, Y. High
32 Performance n-Type Organic Field-Effect Transistors Based on π -Electronic Systems
33 with Trifluoromethylphenyl Groups. *J. Am. Chem. Soc.* **2005**, *127*, 5336–5337. b)
34 Ando, S.; Murakami, R.; Nishida, J.; Tada, H.; Inoue, Y.; Tokito, S.; Yamashita, Y.
35 n-Type Organic Field-Effect Transistors with Very High Electron Mobility Based on
36 Thiazole Oligomers with Trifluoromethylphenyl Groups. *J. Am. Chem. Soc.* **2005**, *127*,
37 14996–14997.
- 38
39
40
41
42
43
44
45
46 12 Liu, J.; Meng, L.; Zhu, W.; Zhang, C.; Zhang, H.; Yao, Y.; Wang, Z.; He, P.; Zhang, X.;
47 Wang, Y.; Zhen, Y.; Dong, H. Yi, Y.; Hu, W. A cross-dipole stacking molecule of an
48 anthracene derivative: integrating optical and electrical properties. *J. Mater. Chem. C*
49 **2015**, *3*, 3068–3071.
- 50
51
52
53
54
55 13 Seidel, N.; Hahn, T.; Liebing, S.; Seichter, W.; Kortus, J.; Weber, E. Synthesis and
56 properties of new 9, 10-anthraquinone derived compounds for molecular electronics.
57 *New J.Chem.* **2013**, *37*, 601–610.
- 58
59
60

- 1
2
3
4
5 14 Grushin, V. V. Fluoroform as a feedstock for high-value fluorochemicals. *Chim. Oggi*
6
7 *Chem. Today* **2014**, *32*, 81–90.
8
9 15 He, L.; Tsui, G. C. Fluoroform-derived CuCF₃ for trifluoromethylation of terminal and
10
11 TMS-protected alkynes. *Org. Lett.* **2016**, *18*, 2800–2803.
12
13 16 Kim, D. W.; Choi, H. Y.; Lee, K. J.; Chi, D. Y. Facile Oxidation of fused 1,
14
15 4-dimethoxybenzenes to 1, 4-quinones using NBS: Fine-tuned Control over
16
17 Bromination and Oxidation Reactions. *Org. Lett.* **2001**, *3*, 445–447.
18
19 17 The commonly used formal potential of the redox couple of ferrocenium/ferrocene
20
21 (Fc⁺/Fc) in the Fermi scale is –5.1 eV, which is calculated on the basis of an
22
23 approximation neglecting solvent effects using a work function of 4.46 eV for the
24
25 normal hydrogen electrode (NHE) and an electrochemical potential of 0.64 V for
26
27 (Fc⁺/Fc) versus NHE. See: Cardona, C. M.; Li, W.; Kaifer, A. E.; Stockdale, D.; Bazan,
28
29 G. C. Electrochemical Considerations for Determining Absolute Frontier Orbital
30
31 Energy Levels of Conjugated Polymers for Solar Cell Applications. *Adv. Mater.* **2011**,
32
33 *23*, 2367–2371.
34
35 18 Liu, D.; He, Z.; Su, Y.; Diao, Y.; Mannsfeld, S. C.; Bao, Z.; Xu, J.; Miao, Q.
36
37 Self-Assembled Monolayers of Cyclohexyl-Terminated Phosphonic Acids as a General
38
39 Dielectric Surface for High-Performance Organic Thin-Film Transistors. *Adv. Mater.*
40
41 **2014**, *26*, 7190–7196.
42
43 19 Jiang, L.; Gao, J.; Wang, E.; Li, H.; Wang, Z.; Hu, W.; Jiang, L. Organic
44
45 single-crystalline ribbons of a rigid “H”-type anthracene derivative and
46
47 high-performance, short-channel field-effect transistors of individual
48
49 micro/nanometer-sized ribbons fabricated by an “organic ribbon mask” technique. *Adv.*
50
51 *Mater.* **2008**, *20*, 2735–2740.
52
53 20 Yang, J.; Dass, A.; Rawashdeh, A. M. M.; Sotiriou-Leventis, C.; Panzner, M. J.; Tyson,
54
55
56
57
58
59
60

- 1
2
3
4 D. S.; Kinde, J. D. ; Leventis, N. Arylethynyl substituted 9, 10-anthraquinones:
5 Tunable stokes shifts by substitution and solvent polarity. *Chem. Mater.* **2004**, *16*,
6 3457–3468.
7
8
9
10
11 21 Bailey, D.; Williams, V. E. An efficient synthesis of substituted anthraquinones and
12 naphthoquinones. *Tetrahedron Lett.* **2004**, *45*, 2511–2513.
13
14
15
16
17
18
19
20
21
22
23
24
25
26
27
28
29
30
31
32
33
34
35
36
37
38
39
40
41
42
43
44
45
46
47
48
49
50
51
52
53
54
55
56
57
58
59
60